ACS APPLIED MATERIALS & INTERFACES

Research Article

Cite This: ACS Appl. Mater. Interfaces 2018, 10, 22453−22459

www.acsami.org

Ligand-Asymmetric Janus Quantum Dots for Efficient Blue-Quantum Dot Light-Emitting Diodes

Ikjun Cho,[†,¶] Heeyoung Jung,[‡,¶] Byeong Guk Jeong,[∥] Donghyo Hahm,[§] Jun Hyuk Chang,[§] Taesoo Lee,[‡] Kookheon Char,[§] Doh C. Lee,[∥] Jaehoon Lim,[⊥] Changhee Lee,[*,‡] Jinhan Cho,[*,†] and Wan Ki Bae[*,#]

[†]Department of Chemical and Biological Engineering, Korea University, Seoul 02841, Republic of Korea

[‡]School of Electrical and Computer Engineering, Inter-University Semiconductor Research Center and [§]School of Chemical and Biological Engineering, The National Creative Research Initiative Center for Intelligent Hybrids, Seoul National University, Seoul 08826, Republic of Korea

[∥]Department of Chemical and Biomolecular Engineering, Korea Advanced Institute of Science and Technology (KAIST), Daejeon 34141, Republic of Korea

[⊥]Department of Chemical Engineering and Department of Energy System Research, Ajou University, Suwon 16499, Republic of Korea

[#]SKKU Advanced Institute of Nano Technology (SAINT), Sungkyunkwan University, Seobu-ro, Jangan-gu, Suwon-si 16419, Gyeonggi-do, Republic of Korea

Supporting Information

ABSTRACT: We present ligand-asymmetric Janus quantum dots (QDs) to improve the device performance of quantum dot light-emitting diodes (QLEDs). Specifically, we devise blue QLEDs incorporating blue QDs with asymmetrically modified ligands, in which the bottom ligand of QDs in contact with ZnO electron-transport layer serves as a robust adhesive layer and an effective electron-blocking layer and the top ligand ensures uniform deposition of organic hole transport layers with enhanced hole injection properties. Suppressed electron overflow by the bottom ligand and stimulated hole injection enabled by the top ligand contribute synergistically to boost the balance of charge injection in blue QDs and therefore the device performance of blue QLEDs. As an ultimate achievement, the blue QLED adopting ligand-asymmetric QDs displays 2-fold enhancement in peak external quantum efficiency (EQE = 3.23%) compared to the case of QDs with native ligands (oleic acid) (peak EQE = 1.49%). The present study demonstrates an integrated strategy to control over the charge injection properties into QDs via ligand engineering that enables enhancement of the device performance of blue QLEDs and thus promises successful realization of white light-emitting devices using QDs.

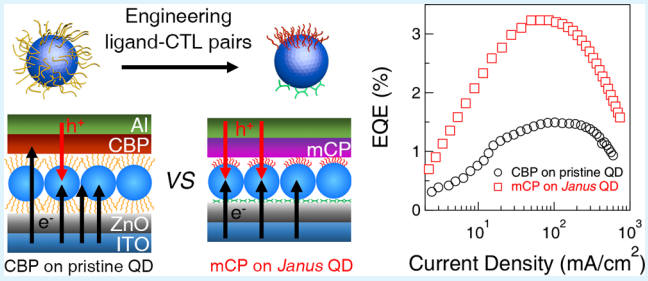

KEYWORDS: *ligand-asymmetric quantum dot, quantum dot-based light-emitting diode, interface engineering, hole transport layer engineering, charge balance*

INTRODUCTION

Nanocrystal quantum dot (QD)-based light-emitting diodes (QLEDs) that generate photons from electrically pumped charge carriers hold key advantages of tunable emission wavelength, narrow emission spectral bandwidth, and excellent intrinsic luminescence efficiency.[1−8] Along with the feasibility of cost-efficient solution processing methods, these features promise QLEDs as the next-generation displays or lightings following commercialized organic or inorganic light-emitting diodes.

High efficiency is prerequisite for practicable use of QLEDs. The device efficiency of QLEDs is determined by the luminance efficiency of QD emissive layers under operation that is reduced by nonradiative recombination processes of injected charge carriers.[9,10] Among reported limiting factors, the presence of excess charge carriers (more than one electron and hole) and subsequent Auger recombination (AR), in which a pair of electron and hole recombines by giving up its energy to third charge carrier,[11,12] is known to be the most daunting for the device efficiency.[8] Since AR is effective to most QDs except few specific cases, circumventing the situation for AR is regarded as the principal approach for improving the device efficiency.[8,13]

Received: May 19, 2018
Accepted: June 7, 2018
Published: June 7, 2018

DOI: 10.1021/acsami.8b08300
ACS Appl. Mater. Interfaces 2018, 10, 22453−22459

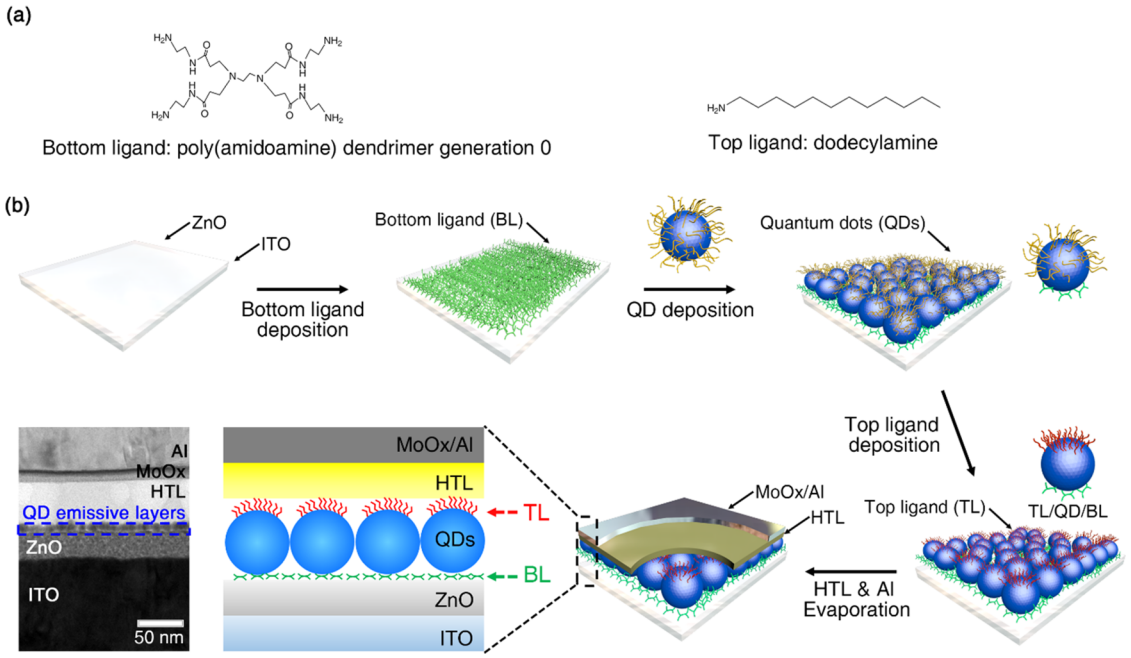

Figure 1. (a) Chemical structures of bottom ligands (poly(amidoamine) dendrimer generation 0, PAD) and top ligands (dodecylamine, DA). (b) Schematic illustration of fabrication process for blue QLED incorporating ligand-asymmetric Janus QDs and its cross-sectional transmission electron microscopy (TEM) image. Bottom ligands (BLs), blue CdZnS/ZnS (core radius (r) = 2.0 nm/shell thickness (h) = 2.3 nm) QDs encapsulated with oleic acid (OA) ligands, and top ligands (TLs) are sequentially spin-casted on ZnO//ITO substrates to yield ligand-asymmetric QD emissive layers. In situ ligand replacement with bottom ligands and top ligands occurs during deposition of QD and the top ligand solutions.

In typical QLEDs, between charge transport layers (CTLs) lies a layer of QDs, which are surrounded by chemical ligands.[2,13−20] In such configuration, the injection rate of charge carriers into QDs is determined not only by the electrical and electronic properties of CTLs[14−18] but also the structure and functionality of ligands.[13,19,20] To maximize the capability of controlling over the charge injection properties, cooperative engineering of ligand and CTL pairs is desired for both electron and hole injection.

Herein, we demonstrate for the first time engineering both sides of ligand and CTL pair, to improve the charge injection balance in QDs and the device performance of QLEDs. Specifically, we devise blue QLEDs incorporating ligand-asymmetric Janus quantum dots (QDs), in which the bottom ligand (BL) of QDs in contact with ZnO electron-transport layer (ETL) serves as an effective electron-blocking layer and the top ligand (TL) ensures uniform deposition of organic hole transport layer (HTL) with the enhanced hole injection property. As a synergistic effect of suppressed electron overflow by BL−ETL pair and stimulated hole injection enabled by TL−HTL pair, blue QLED implementing engineered ligand−CTL pairs exhibits 2-fold enhancement in device efficiency compared to the reference QLED. The present study demonstrates a comprehensive strategy to control over the charge injection properties into QDs and also offers an effective platform for realization of wide-ranging optoelectronic applications using QDs.

RESULTS AND DISCUSSION

The up-to-date QLED with the record efficiency adopts hybrid CTLs (metal oxide electron-transport layer (ETL) and organic hole transport layer (HTL)) that transport charge carriers to QD emissive layers.[6,9,16,21] In QLEDs with hybrid CTLs, the conduction band edge energy level of QDs is close to that of metal oxide ETL, whereas the valance band edge (VBE) energy levels of QDs reside deeper (>0.6 eV) than highest occupied molecular orbital (HOMO) energy levels of organic HTLs.[16] The difference in energy level off-sets leads to unbalanced charge carrier injection into QDs and readily yields accumulation of excess electrons in QDs, which elevates the possibility of nonradiative AR in QD emissive layers and consequently reduces the device efficiency.[8,9,13] The asymmetry in energy level off-sets becomes greater for QLEDs with large bandgap QDs whose VBE energy levels reside deeper (Figure S1), which exacerbates the charge imbalance in QDs and thereby the device efficiency.[16,22] To alleviate the charge injection imbalance into QD emissive layers in blue QLEDs, the capability of controlling both electron and hole injection rates is required. Given that the charge injection rates into QDs are determined both by the electrical and electronic properties of CTLs[14−18] and the structure and functionality of ligands,[13,19,20] engineering ligands in chorus with CTLs is expected to provide wider flexibility in adjusting charge injection rates. In addition, integrated engineering of both sides of ligand−CTL pair will improve the charge injection balance within QDs and thus benefit the device efficiency.

In the present study, we offer an integrated approach, in which ligands on either side of QDs are tailored. The legitimacy of the new strategy is examined in the context of balanced charge injection into QD layers and its effect on the device performance of QLEDs. With the aim of individual control of electron and hole injection properties, we have designed ligand-asymmetric Janus QDs, in which two distinct ligands partition the surface of QDs and independently contribute to engineer the charge injection rates. As a model system, we have implemented CdZnS/ZnS (core radius (r) = 2.0 nm/shell thickness (h) = 2.3 nm) core/shell blue QDs[23] with asymmetrically modified ligands in an inverted QLED

DOI: 10.1021/acsami.8b08300
ACS Appl. Mater. Interfaces 2018, 10, 22453−22459

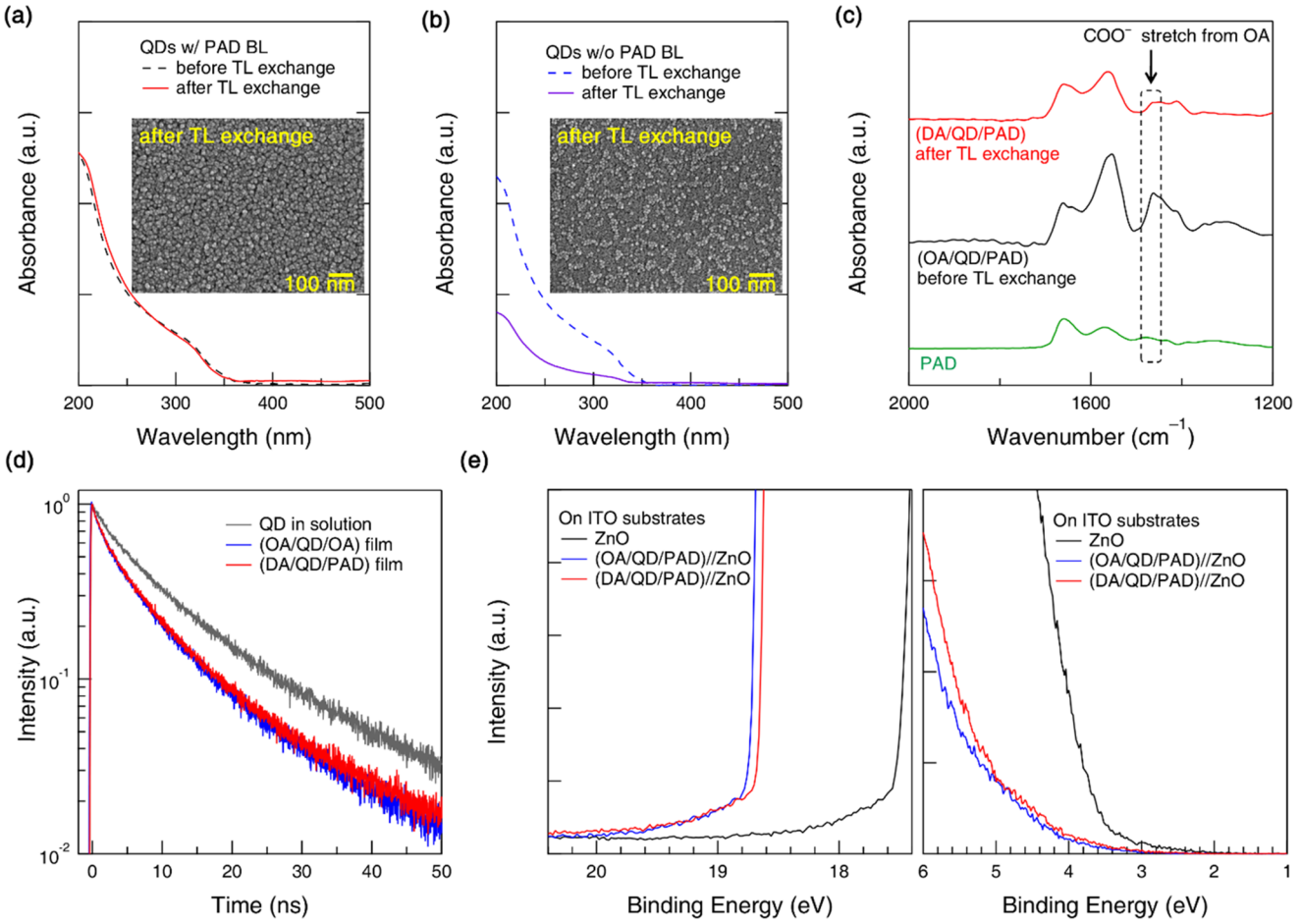

Figure 2. Characteristics of QD emissive layers upon ligand exchange processes. UV−vis spectra of QD films before (broken line) and after (solid line) DA top ligand (DA TL) replacement (a) with and (b) without PAD bottom ligand. The insets show the scanning electron microscope images of QD films after top ligand (DA) replacement (inset (a)) with PAD BL (DA/QD/PAD) and (inset (b)) without PAD BL (DA/QD/OA) on ZnO layer. (c) FT-IR spectra of PAD, QD emissive layers on PAD (i.e., before TL exchange, (OA/QD/PAD)), and ligand-asymmetric QD emissive layers (i.e., after TL exchange, (DA/QD/PAD)). The absorption intensity corresponding to COO^- symmetric stretching peak (1459 cm^{-1}) of native ligands (OA) decreases after deposition of primary aliphatic amine (i.e., DA) TLs. (d) PL decay dynamics of QD films with OA ligands ((OA/QD/OA) film, blue) versus with asymmetric ligands ((DA/QD/PAD) film, red). PL decay dynamics of OA-stabilized QD solution (OA−QD in solution, dark gray) is overlaid for comparison. (e) Ultraviolet photoelectron spectra (UPS) at the high binding energy region (left) and at the low binding energy region (right) of ZnO (black), (OA/QD/PAD)//ZnO (blue), and (DA/QD/PAD)//ZnO (red) on ITO substrates.

with hybrid CTLs (Figures 1 and S2). More specifically, the bottom surface of QD layer bound to the ZnO ETL is mainly passivated with primary amine-functionalized poly(amidoamine) dendrimer (PAD) ligand, whereas the top surface of QD layer in contact with HTL is mainly stabilized with dodecylamine (DA) ligands (Figures 2 and S3). These ligand-asymmetric Janus QDs are fabricated by sequential spin-casting of PAD bottom ligand (BL), oleic acid-stabilized QD (OA−QD), and DA top ligand (TL) solutions on ZnO ETL. We note that the ligand replacement leaves residual OA whose ratios remaining on the bottom and top surface of the resultant QD layer are calculated to be approximately 7 and 27%, respectively (Figure S3). Organic HTL, MoOx hole injection layer, and Al electrode are thermally evaporated on top of Janus QDs//ZnO//ITO to complete inverted blue QLEDs with hybrid CTLs.

Thanks to the presence of dendrimer type BLs that link both ZnO ETL and QDs, the QD emissive layer preserves its morphology during TL deposition process (Figure 2a−c). Multiple steps of ligand replacement do not alter photophysical and electronic properties of CdZnS QD emissive cores (Figure 2d,e), enabling us to characterize the influence of engineered ligand−CTL pairs on the charge injection properties into QDs and the device performance. Instead, a PAD BL−ZnO ETL pair alters the energy levels of ZnO and consequently adjusts the rates of electron injection from ZnO ETL into QDs. The primary amine groups that coordinate to Zn atoms at the surface of ZnO shift up the electronic energy level of ZnO by at most 0.5 eV (Figure S4 and Table S1),[13,24] which impedes electron injection from ZnO ETL into the QDs.

Together with the suppression of electron overflow by the insertion of amine-functionalized BLs, stimulating the hole injection is expected to further enhance the charge balance and thereby the device efficiency. For that purpose, we have engineered optoelectronic properties of organic HTLs (Figure S5). The hole injection rate is closely related to the energy level off-set between VBE of QDs and HOMO of HTLs. To minimize the energy barrier for hole injection, we could narrow candidates among commercialized organic HTLs down to 1,3-bis(*N*-carbazolyl)benzene (mCP)[25] and 4,4′-bis(*N*-carbazolyl)-1,1′-biphenyl (CBP)[26] whose HOMO energy levels are as low as 6.0 eV (Figure S5). Except the similarity in HOMO

DOI: 10.1021/acsami.8b08300
ACS Appl. Mater. Interfaces 2018, 10, 22453−22459

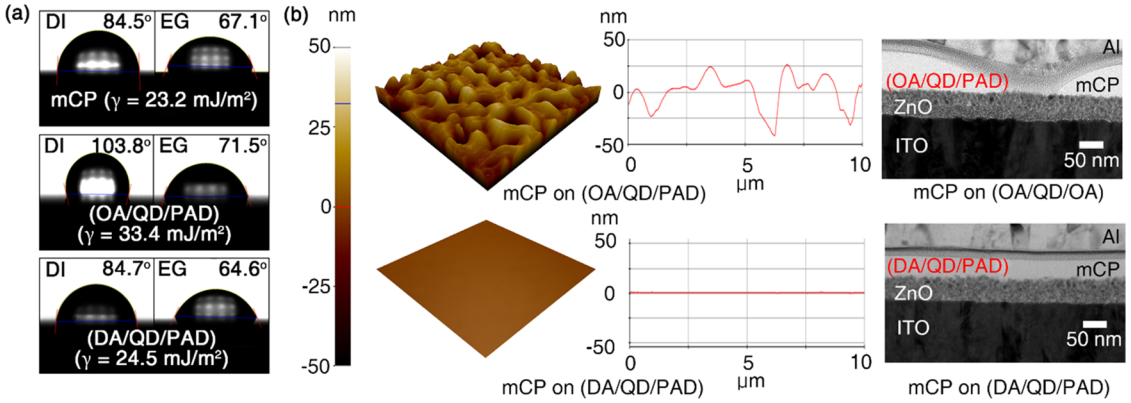

Figure 3. Role of top ligands on the morphology of thermally evaporated hole transport layer (mCP) and corresponding device characteristics. (a) Contact angle images with deionized water (left) and ethylene glycol (right) and the calculated surface energy (γ) of mCP (top) and QD films before top ligand exchange ((OA/QD/PAD), middle) and after top ligand exchange ((DA/QD/PAD), bottom) films. (b) Atomic force microscopy images (left) and their height profiles (middle, scan range: 10 μm × 10 μm) of mCP layers evaporated on QDs with OA (mCP on (OA/QD/PAD), up) and DA (mCP on (DA/QD/PAD), down). Cross-sectional TEM images (right) of QLEDs incorporating mCP (right) on QDs with native top ligands (mCP on (OA/QD/PAD), up) versus exchanged top ligands (mCP on (DA/QD/PAD), down).

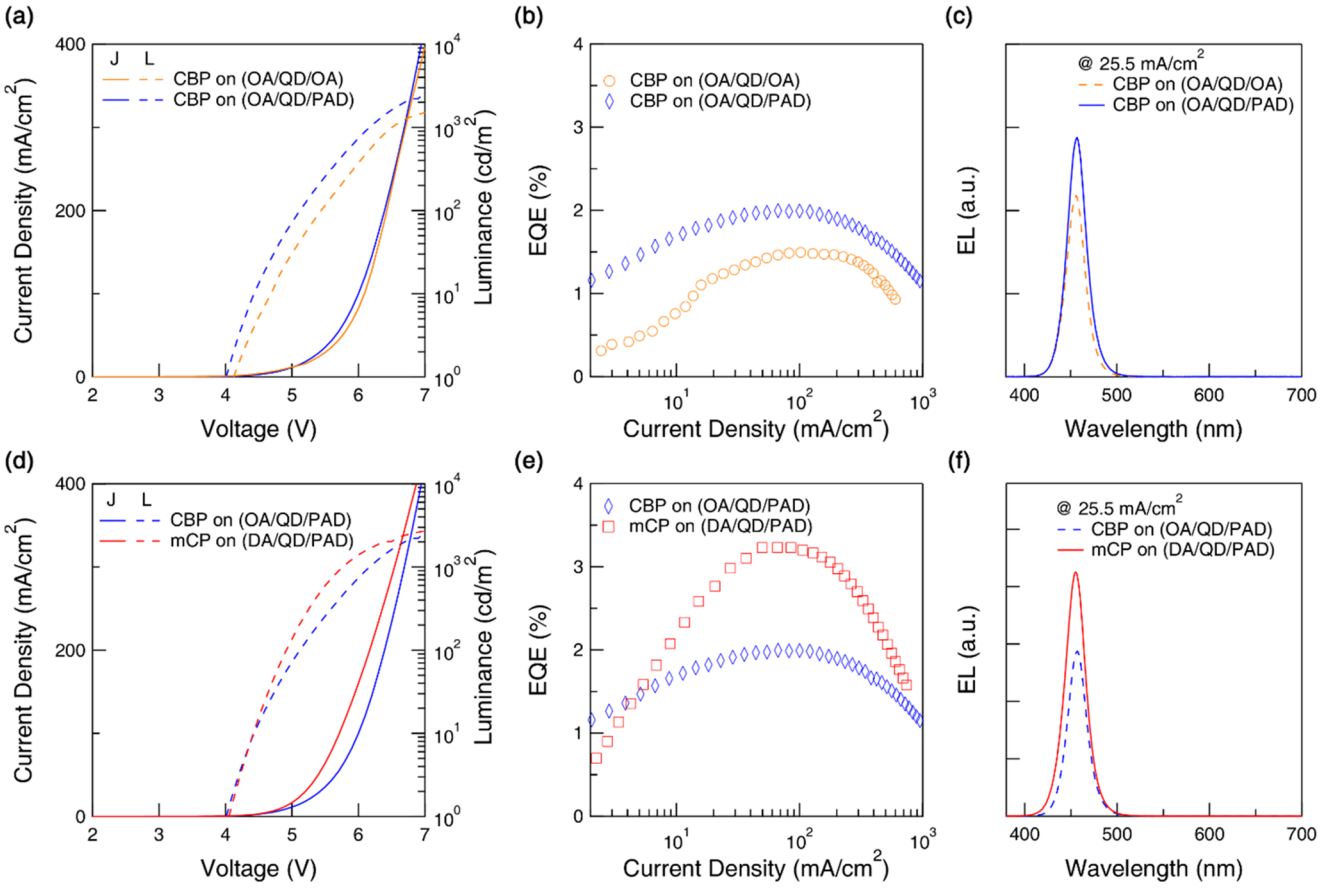

Figure 4. Synergistic effects of the bottom ligand and the top ligand on the efficiency enhancement of blue QLEDs. (a, d) Current density–voltage–luminance characteristics, (b, e) external quantum efficiency (EQE) versus current density, and (c, f) electroluminescence spectra (at a current density of 25.5 mA/cm^2) of QLEDs with (a–c) CBP on (OA/QD/OA) (orange) versus (OA/QD/PAD) (blue) and (d–f) CBP on (OA/QD/PAD) (blue) versus mCP on (DA/QD/PAD) (red).

energy levels, mCP and CBP hold different electrical and electronic properties, including hole mobility (ca. ~1.2 × 10^{-4} cm^2/(V s) for mCP[27] and ~1 × 10^{-3} cm^2/(V s) for CBP[16]) and lowest unoccupied molecular orbital (LUMO) energy levels (Figure S5), and therefore direct comparison of the device performance of QLEDs employing mCP versus CBP is expected to hint important parameters in controlling the hole injection rate.

mCP contrasts with CBP with respect to not only the electrical and electronic properties but also the surface energy (Figures 3 and S6). Contrary to the case with CBP, the substantial difference in the surface energy between mCP and oleic acid (OA)-capped QDs ($\Delta\gamma$ = 10.2 mJ/m^2) deters

DOI: 10.1021/acsami.8b08300
ACS Appl. Mater. Interfaces 2018, 10, 22453–22459

Table 1. Device Characteristics of QLEDs Employing CdZnS(r = 2 nm)/ZnS(h = 2.3 nm) Blue-Emitting QD Emissive Layers with CBP (CBP on (OA/QD/OA) and CBP on (OA/QD/PAD)) versus mCP (mCP on (OA/QD/OA) and (DA/QD/PAD))[a]

HTL	QDs	λ_{max}	V_{ON}	max EQE (%)	max CE (cd/A)	max PE (lm/W)	L (cd/m^2)@25 (mA/cm^2)
CBP	(OA/QD/OA)	456	3.3	1.49	0.45	0.24	90.7
	(OA/QD/PAD)	457	3.2	1.99	0.74	0.41	159.2
mCP	(OA/QD/OA)	456	3.3	0.07	0.02	0.01	5.6
	(DA/QD/PAD)	455	3.1	3.23	1.08	0.61	272.1

[a]Abbreviations: wavelength of maximum EL peak intensities (λ_{max}), turn-on voltage (V_{ON}), current efficiency (CE), power efficiency (PE), and luminance (L).

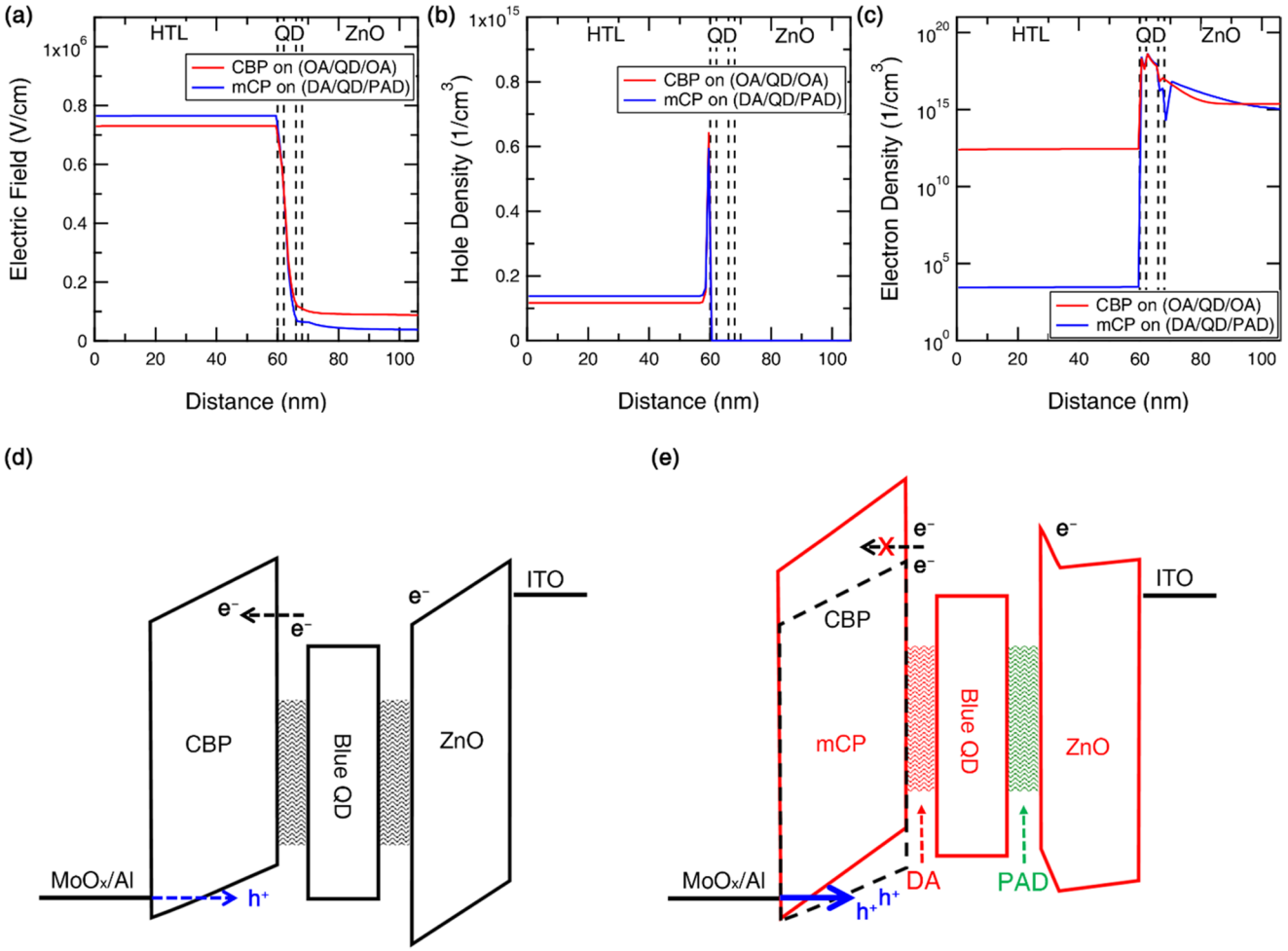

Figure 5. (a–c) Simulation results at 5 V and (d, e) proposed mechanism for the efficiency enhancement in the blue QLED employing mCP on ligand-asymmetric Janus QDs. (a) Electric field, (b) hole density, and (c) electron density in blue QLEDs employing mCP on ligand-asymmetric QDs (mCP on (DA/QD/PAD), red solid line) versus native ligand QDs (CBP on (OA/QD/OA), blue dotted line). Energy band diagrams of blue QLED employing (d) CBP on QDs with native ligands (i.e., (OA/QD/OA)) versus (e) mCP on ligand-asymmetric QDs (i.e., (DA/QD/PAD)).

homogenous formation of mCP films on QD emissive layers, leading to the growth of mCP in islands and holes structure that cause current leakage centers in QLEDs (Figure S7). By contrast, modification of TLs of QDs with DA whose surface energy is commensurate with that of mCP film ($\Delta\gamma$ = 1.3 mJ/m^2) leads to uniform growth of mCP layers (Figure 3a,b). The resulting blue QLED adopting mCP on ligand-asymmetric Janus QDs exhibits 2-fold enhancement in current density and peak external quantum efficiency (EQE = 3.23%) compared to the reference QLED implementing CBP on QDs with native ligands (EQE = 1.49%). The increase in both the current density and the device efficiency is attributed to the enhanced hole injection into QDs by mCP that improves the charge balance in QDs and thereby their luminance efficiency. We note that the EQE of 3.23% is a record high value among inverted blue QLEDs with hybrid CTLs.

To better understand the role of ligand–CTL pairs on the device performance, we have conducted comparative study on QLEDs with varying combinations of ligand–CTL pairs (Figure 4 and Table 1). The PAD–ZnO ETL pair enhances the luminance efficiency without altering the current density of QLEDs (Figure 4a–c), indicating that PAD enhances the charge balance in QD emissive layers by suppressing the electron overflow from ZnO into QDs. By contrast, the DA–mCP pair leads to the increase in both the current density and the EL efficiency of QLED compared with the case of OA–

DOI: 10.1021/acsami.8b08300
ACS Appl. Mater. Interfaces 2018, 10, 22453–22459

CBP or DA−CBP pair (Figures 4d−f and S8), suggesting that mCP enhances the balance of charge carriers within QDs by promoting the hole injection into QDs in spite of its lower mobility compared to that of CBP.

The intrinsic hole mobility of HTL barely rationalizes the substantial enhancement in hole injection rate of QLED employing mCP. Instead, difference in the electric field across QLED accounts for the enhanced hole injection rates (Figure 5). The LUMO energy level of mCP resides upper (~0.6 eV) than that of CBP, which effectively blockades electron leakage into HTLs. The accumulated electrons at the interface between mCP and TLs promote the hole injection from electrodes into HTL by increasing the electric field across HTL layer,[28] leading to the increase in the hole density in HTL nearby QD emissive layers that stimulate the hole injection from HTL into QDs (Figure 5a,b). In addition, the accumulated electrons decrease the electric field across ZnO and help to reduce the electron injection rate (Figure 5a,c). The introduction of PAD on ZnO creates an energetic barrier for electron injection, which further enhances charge balance in QDs. Therefore, both ligand−CTL pairs that simultaneously suppress electron injection and promote hole injection synergistically contribute to enhancement of the charge balance in QDs and hence the device efficiency.

The present study validates the importance of charge injection balance within QD emissive layers to QLED efficiency. We note that despite the significant improvement in the charge injection balance, the record device efficiency achieved in this study (EQE = 3.23%) is still far below the calculated maximum device efficiency (est. EQE = 8%) from the film PL QY (40%). The significant difference between apparent EQE versus the expected limit implies that the charge injection imbalance is still substantial in the present system. We believe that continuing efforts in materials development and device optimization will advance the device performance and eventually enable us to realize efficient blue QLEDs suitable for practicable applications in displays and lightings.

CONCLUSIONS

In summary, we have demonstrated an integrated approach, customizing both sides of ligands in concert with CTLs, to enhance the charge injection balance into QD emissive layers. Each side of ligands plays different roles in controlling the charge injection rates on this platform. Specifically, BLs directly alter the electronic energy levels of ZnO ETL and TLs enabling systematic engineering of HTLs that change the electric field across the device. As a synergistic effect of suppressed electron injection rate and stimulated hole injection rate, blue QLED with engineered ligand−CTL pairs displays substantial enhancement in the device efficiency compared with the reference QLED. The present study validates the importance of charge balance in QLED efficiency and also offers an effective platform that capitalizes on influence of ligands on CTLs for enhancement of charge injection balance and thereby the device efficiency.

ASSOCIATED CONTENT

Supporting Information

The Supporting Information is available free of charge on the ACS Publications website at DOI: 10.1021/acsami.8b08300.

Synthetic methods of QDs and ZnO nanoparticles (chemicals, preparation of precursors, synthesis of QDs, and ZnO nanoparticles), film characterization (PL decay dynamics, Fourier transform infrared spectroscopy (FT-IR), atomic force microscopy (AFM), ultraviolet photoelectron spectroscopy (UPS), and contact angle measurement), device fabrication and characterization, and device simulations are included (PDF)

AUTHOR INFORMATION

Corresponding Authors

*E-mail: jinhan71@korea.ac.kr (J.C.).
*E-mail: wkbae@skku.edu (W.K.B.).
*E-mail: chlee7@snu.ac.kr (C.L.).

ORCID

Heeyoung Jung: 0000-0001-6094-3498
Byeong Guk Jeong: 0000-0002-0544-364X
Kookheon Char: 0000-0002-7938-8022
Doh C. Lee: 0000-0002-3489-6189
Changhee Lee: 0000-0003-2800-8250
Jinhan Cho: 0000-0002-7097-5968
Wan Ki Bae: 0000-0002-3832-2449

Author Contributions

¶I.C. and H.J. contributed equally. The manuscript was written through contributions of all authors. All authors have given approval to the final version of the manuscript.

Notes

The authors declare no competing financial interest.

ACKNOWLEDGMENTS

This work was supported by the Industrial Core technology development program (10077471) funded by the Ministry of Trade, Industry & Energy of Korea. J.C. acknowledges Samsung Research Funding Center of Samsung Electronics under Project Number SRFC-MA1301-07. D.C.L. acknowledges the National Research Foundation (NRF) grants funded by the Korean government (NRF-2016M3A7B4910618).

REFERENCES

(1) Colvin, V. L.; Schlamp, M. C.; Alivisatos, A. P. Light-Emitting Diodes Made from Cadmium Selenide Nanocrystals and a Semiconducting Polymer. *Nature* **1994**, *370*, 354−357.

(2) Coe, S.; Woo, W.-K.; Bawendi, M.; Bulovic, V. Electroluminescence from Single Monolayers of Nanocrystals in Molecular Organic Devices. *Nature* **2002**, *420*, 800−803.

(3) Bae, W. K.; Brovelli, S.; Klimov, V. I. Spectroscopic Insights into the Performance of Quantum Dot Light-Emitting Diodes. *MRS Bull.* **2013**, *38*, 721−730.

(4) Chang, J. H.; Hahm, D.; Char, K.; Bae, W. K. Interfacial Engineering of Core/Shell Heterostructured Nanocrystal Quantum Dots for Light-Emitting Applications. *J. Inf. Disp.* **2017**, *18*, 57−65.

(5) Talapin, D. V.; Lee, J. S.; Kovalenko, M. V.; Shevchenko, E. V. Prospects of Colloidal Nanocrystals for Electronic and Optoelectronic Applications. *Chem. Rev.* **2010**, *110*, 389−458.

(6) Dai, X.; Zhang, Z.; Jin, Y.; Niu, Y.; Cao, H.; Liang, X.; Chen, L.; Wang, J.; Peng, X. Solution-Processed, High-Performance Light-Emitting Diodes Based on Quantum Dots. *Nature* **2014**, *515*, 96−99.

(7) Lim, J.; Jeong, B. G.; Park, M.; Kim, J. K.; Pietryga, J. M.; Park, Y.-S.; Klimov, V. I.; Lee, C.; Lee, D. C.; Bae, W. K. Influence of Shell Thickness on the Performance of Light-Emitting Devices Based on $CdSe/Zn_{1-x}Cd_xS$ Core/Shell Heterostructured Quantum Dots. *Adv. Mater.* **2014**, *26*, 8034−8040.

(8) Bae, W. K.; Park, Y.-S.; Lim, J.; Lee, D.; Padilha, L. A.; McDaniel, H.; Robel, I.; Lee, C.; Pietryga, J. M.; Klimov, V. I. Controlling the

influence of Auger recombination on the performance of quantum-dot light-emitting diodes. *Nat. Commun.* **2013**, *4*, No. 2661.
(9) Pietryga, J. M.; Park, Y.-S.; Lim, J.; Fidler, A. F.; Bae, W. K.; Brovelli, S.; Klimov, V. I. Spectroscopic and Device Aspects of Nanocrystal Quantum Dots. *Chem. Rev.* **2016**, *116*, 10513−10622.
(10) Shirasaki, Y.; Supran, G. J.; Bawendi, M. G.; Bulovic, V. Emergence of Colloidal Quantum-Dot Light-Emitting Technologies. *Nat. Photonics* **2013**, *7*, 13−23.
(11) Klimov, V. I.; Mikhailovsky, A. A.; McBranch, D. W.; Leatherdale, C. A.; Bawendi, M. G. Quantization of Multiparticle Auger Rates in Semiconductor Quantum Dots. *Science* **2000**, *287*, 1011−1013.
(12) Klimov, V. I. Spectral and Dynamical Properties of Multiexcitons in Semiconductor Nanocrystals. *Annu. Rev. Phys. Chem.* **2007**, *58*, 635−675.
(13) Cho, I.; Jung, H.; Jeong, B. G.; Chang, J. H.; Kim, Y.; Char, K.; Lee, D. C.; Lee, C.; Cho, J.; Bae, W. K. Multifunctional Dendrimer Ligands for High-Efficiency, Solution-Processed Quantum Dot Light-Emitting Diodes. *ACS Nano* **2017**, *11*, 684−692.
(14) Mueller, A. H.; Petruska, M. A.; Achermann, M.; Werder, D. J.; Akhadov, E. A.; Koleske, D. D.; Hoffbauer, M. A.; Klimov, V. I. Multicolor Light-Emitting Diodes Based on Semiconductor Nanocrystals Encapsulated in GaN Charge Injection Layers. *Nano Lett.* **2005**, *5*, 1039−1044.
(15) Caruge, J.-M.; Halpert, J. E.; Bulovic, V.; Bawendi, M. G. NiO as an Inorganic Hole-Transporting Layer in Quantum-Dot Light-Emitting Devices. *Nano Lett.* **2006**, *6*, 2991−2994.
(16) Kwak, J.; Bae, W. K.; Lee, D.; Park, I.; Lim, J.; Park, M.; Cho, H.; Woo, H.; Yoon, D. Y.; Char, K.; Lee, S.; Lee, C. Bright and Efficient Full-Color Colloidal Quantum Dot Light-Emitting Diodes Using an Inverted Device Structure. *Nano Lett.* **2012**, *12*, 2362−2366.
(17) Ding, K.; Chen, H.; Fan, L.; Wang, B.; Huang, Z.; Zhuang, S.; Hu, B.; Wang, L. Polyethylenimine Insulativity-Dominant Charge-Injection Balance for Highly Efficient Inverted Quantum Dot Light-Emitting Diodes. *ACS Appl. Mater. Interfaces* **2017**, *9*, 20231−20238.
(18) Ji, W.; Lv, Y.; Jing, P.; Zhang, H.; Wang, J.; Zhang, H.; Zhao, J. Highly Efficient and Low Turn-On Voltage Quantum Dot Light-Emitting Diodes by Using a Stepwise Hole-Transport Layer. *ACS Appl. Mater. Interfaces* **2015**, *7*, 15955−15960.
(19) Shen, H.; Cao, W.; Shewmon, N. T.; Yang, C.; Li, L. S.; Xue, J. High-Efficiency, Low Turn-on Voltage Blue-Violet Quantum-Dot-Based Light-Emitting Diodes. *Nano Lett.* **2015**, *15*, 1211−1216.
(20) Kwak, J.; Bae, W. K.; Zorn, M.; Woo, H.; Yoon, H.; Lim, J.; Kang, S. W.; Wever, S.; Butt, H.-J.; Zentel, R.; Lee, S.; Char, K.; Lee, C. Characterization of Quantum Dot/Conducting Polymer Hybrid Films and Their Application in Light-Emitting Diodes. *Adv. Mater.* **2009**, *21*, 5022−5026.
(21) Yang, Y.; Zheng, Y.; Cao, W.; Titov, A.; Hyvonen, J.; Manders, J. R.; Xue, J.; Holloway, P. H.; Qian, L. High-Efficiency Light-Emitting Devices based on Quantum Dots with Tailored Nanostructures. *Nat. Photonics* **2015**, *9*, 259−266.
(22) Bae, W. K.; Lim, J.; Lee, D.; Park, M.; Lee, H.; Kwak, J.; Char, K.; Lee, C.; Lee, S. R/G/B/Natural White Light Thin Colloidal Quantum Dot-Based Light-Emitting Devices. *Adv. Mater.* **2014**, *26*, 6387−6393.
(23) Bae, W. K.; Nam, M. K.; Char, K.; Lee, S. Gram-Scale One-Pot Synthesis of Highly Luminescent Blue Emitting $Cd_{1-x}Zn_xS$/ZnS Nanocrystals. *Chem. Mater.* **2008**, *20*, 5307−5313.
(24) Zhou, Y.; Fuentes-Hernandez, C.; Shim, J.; Meyer, J.; Giordano, A. J.; Li, H.; Winget, P.; Papadopoulos, T.; Cheun, H.; Kim, J.; Fenoll, M.; Dindar, A.; Haske, W.; Najafabadi, E.; Khan, T. M.; Sojoudi, H.; Barlow, S.; Graham, S.; Bredas, J.-L.; Marder, S. R.; Kahn, A.; Kippelen, B. A Universal Method to Produce Low-Work Function Electrodes for Organic Electronics. *Science* **2012**, *336*, 327−332.
(25) Adamovich, V.; Brooks, J.; Tamayo, A.; Alexander, A. M.; Djurovich, P. I.; D'Andrade, B. W.; Adachi, C.; Forrest, S. R.; Thompson, M. E. High Efficiency Single Dopant White Electrophosphorescent Light Emitting Diodes. *New J. Chem.* **2002**, *26*, 1171−1178.
(26) Koene, B. E.; Loy, D. E.; Thompson, M. E. Asymmetric Triaryldiamines as Thermally Stable Hole Transporting Layers for Organic Light-Emitting Devices. *Chem. Mater.* **1998**, *10*, 2235−2250.
(27) Wu, M.-F.; Yeh, S.-J.; Chen, C.-T.; Murayama, H.; Tsuboi, T.; Li, W.-S.; Chao, I.; Liu, S.-W.; Wang, J.-K. The Quest for High-Performance Host Materials for Electrophosphorescent Blue Dopants. *Adv. Funct. Mater.* **2007**, *17*, 1887−1895.
(28) Ruhstaller, B.; Carter, S. A.; Barth, S.; Riel, H.; Riess, W.; Scott, J. C. Transient and Steady-State Behavior of Space Charges in Multilayer Organic Light-Emitting Diodes. *J. Appl. Phys.* **2001**, *89*, 4575−4586.

DOI: 10.1021/acsami.8b08300
ACS Appl. Mater. Interfaces 2018, 10, 22453−22459